



The effect of transverse normal strain in contact of an orthotropic beam pressed against a circular surface

Amir Gasmi^a, Paul F. Joseph^{a,*}, Timothy B. Rhyne^b, Steven M. Cron^b

^a Department of Mechanical Engineering, Clemson University, Fluor Daniel Building, Clemson, SC 29634, USA

^b Michelin Americas Research and Development Company, 515 Michelin Road Greenville, SC 29605, USA

ARTICLE INFO

Article history:

Received 17 January 2012

Received in revised form 20 April 2012

Available online 6 June 2012

Keywords:

Contact mechanics

Beam theory

Orthotropic material

Transverse normal strain

Timoshenko beam theory

ABSTRACT

The contact problem of a straight orthotropic beam pressed onto a rigid circular surface is considered using beam theories that account for transverse shear and transverse normal deformations. The circular nature of the rigid surface emphasizes the difference between Euler Bernoulli theory behavior, where point loads develop at the edge of contact, and the higher order theories that predict non-singular pressure distributions. While Timoshenko beam theory is the simplest theory that addresses this behavior, the prediction of a maximum value of pressure at the edge of contact contradicts the elasticity theory result that contact pressure must drop to zero. Transverse normal strain is therefore introduced, both to study this fundamental discrepancy and to include an important effect in many contact problems. To investigate this effect, higher order beam theories that account for both constant and linear transverse normal strain through the beam thickness are derived using the principle of virtual work. The resulting orthotropic beam theories depend on the bending stiffness (EI), shear stiffness (GA), axial stiffness (EA_1) and transverse normal stiffness (EA_2), which are independent stiffness parameters that can differ by orders of magnitude. The above mentioned contact problem is then solved analytically for these theories, along with the Timoshenko beam model which assumes zero transverse normal strain. The results for different orthotropic materials show that inclusion of transverse normal deformation has a significant effect on the contact pressure solution. Furthermore, the solution using higher order beam theories encompasses the two extremes of a Hertz-like contact pressure when the half contact length is smaller than the thickness of the beam, and the Timoshenko beam theory case when the half contact length is much larger than the thickness. Concerning the behavior of the pressure at the edge of contact, adherence to the boundary conditions required by the principle of virtual work, shows that while the pressure does tend to zero, it does not become zero unless artificially enforced. In this regard the solution for the case of linear strain is better than that for constant strain. All beam solutions are validated with plane elasticity solutions obtained using the commercial finite element software ABAQUS.

© 2012 Elsevier Ltd. All rights reserved.

1. Introduction

Although Euler–Bernoulli and Timoshenko beam theories have proven to be sufficient and efficient in describing the behavior of structural elements for different types of loading, these elementary theories exhibit inconsistency in problems involving contact (Essenburg, 1975; Naghdi and Rubin, 1989). According to Essenburg (1975) and Naghdi and Rubin (1989), the inclusion of transverse normal deformation, in addition to local transverse shear deformation, should be accounted for in contact problems of thin structures. In a later study, Hodges (2003) showed that, by including the effects of warping of the cross-section of the beam

using a formulation derived from Euler–Lagrange equations, this inconsistency can be removed without having to consider transverse normal strain. From the computational point of view, El-Abbasi and Meguid (1999) showed that by including transverse normal deformation of a shell, the derived large deformation finite elements are capable of accurately simulating contact problems involving shell structures. The formulation was tested theoretically and experimentally using various examples.

The behavior of the contact stress at the edge of contact is of interest, since the elementary theories do not predict that the stress drops to zero as required by elasticity theory (see, for example, Johnson (1985)). Essenburg (1975) and Naghdi and Rubin (1989) took advantage of the flexibility provided by including the transverse normal strain to force this behavior. Similarly, Hodges (2003) requires the contact stress to be continuous using a slack variable approach.

* Corresponding author. Tel.: +1 864 656 0545.

E-mail address: jpaul@clemson.edu (P.F. Joseph).

In this paper, the affect of including normal deformation through the thickness in contact problems of thin structures will be addressed by using the principle of virtual work. In particular, the effect of transverse normal strain, which is taken as constant and linear through the thickness, on the behavior of the contact stress at the edge of contact will be investigated. The problem of a straight beam brought into contact with a rigid circular surface, as considered by Keer and Silva (1970), will be used in the current study. All of the previously mentioned studies apply to isotropic material behavior. In this paper, in addition to accounting for transverse normal strain, the orthotropic character of the beam is taken into account. This flexibility is required to address problems where transverse normal strain is expected to be significant, such as a beam with a soft compliant layer on its contacting surface.

2. Formulation and governing equations

Consider a one-dimensional model of a straight beam as illustrated by Fig. 1. The rectangular cross-section is defined by its thickness h and its out-of-plane width b as shown in Fig. 1. In the subsequent sections, the development of the higher order beam theory for quadratic displacement through the thickness, i.e. linear normal strain in the y -direction, is considered using the principle of virtual work. The constant and zero strain cases are then easily obtained from the governing equations.

2.1. Quadratic beam theory

In this subsection the beam formulation is based on the assumption that the transverse component of displacement vector field is expanded in a quadratic polynomial expression with respect to the thickness variable, while the axial component of the displacement vector field is expanded in a linear polynomial expression with respect to the thickness variable.

2.1.1. Equilibrium equations

Consider the following approximation of the displacement field with respect to the thickness coordinate,

$$\begin{aligned} u_x(x, y) &= u(x) + y\phi(x), \\ u_y(x, y) &= w(x) + y\psi(x) + y^2\beta(x). \end{aligned} \quad (1)$$

This physically-based approach is selected for the following two reasons: (1) it is the most direct way to study the importance of transverse normal strain in contact problems and (2) it is the best choice for an orthotropic beam where the orders of magnitude of the stiffness parameters are not necessarily the same. In linear elasticity, i.e. infinitesimal deformation and small deflection, the standard expressions for strain in Cartesian coordinates are given by,

$$\varepsilon_{xx} = \frac{\partial u_x}{\partial x}, \quad \varepsilon_{yy} = \frac{\partial u_y}{\partial y}, \quad \gamma_{xy} = 2\varepsilon_{xy} = \frac{\partial u_x}{\partial y} + \frac{\partial u_y}{\partial x}. \quad (2)$$

Substituting (1) into (2) yields,

$$\varepsilon_{xx} = \frac{du}{dx} + y\frac{d\phi}{dx}, \quad \varepsilon_{yy} = \psi + 2y\beta, \quad \gamma_{xy} = \phi + \frac{dw}{dx} + y\frac{d\psi}{dx} + y^2\frac{d\beta}{dx}. \quad (3)$$

This shows that the displacement expressions (1) result in transverse normal strain that is linear with respect to the thickness

coordinate, and that ψ can be interpreted as the average transverse strain of the cross-section. Furthermore, the shear strain is a quadratic function of the thickness coordinate due to the contribution of the function β from Eq. (1)₂.

The virtual strain energy for the straight continuum strip defined in Fig. 1, is given by,

$$\begin{aligned} \delta U &= \int_{\Omega} (\sigma_{xx}\delta\varepsilon_{xx} + \sigma_{yy}\delta\varepsilon_{yy} + \tau_{xy}\delta\gamma_{xy})d\Omega \\ &= \int_{x_1}^{x_2} \int_A (\sigma_{xx}\delta\varepsilon_{xx} + \sigma_{yy}\delta\varepsilon_{yy} + \tau_{xy}\delta\gamma_{xy})dAdx. \end{aligned} \quad (4)$$

Substituting the strain expressions (3) into (4) yields,

$$\begin{aligned} \delta U &= \int_{x_1}^{x_2} \int_A \left[\sigma_{xx}\delta\left(\frac{du}{dx} + y\frac{d\phi}{dx}\right) + \sigma_{yy}\delta(\psi + 2y\beta) \right. \\ &\quad \left. + \tau_{xy}\delta\left(\phi + \frac{dw}{dx} + y\frac{d\psi}{dx} + y^2\frac{d\beta}{dx}\right) \right] dAdx \\ &= \int_{x_1}^{x_2} \int_A \left[\sigma_{xx}\frac{d\delta u}{dx} + \left(y\sigma_{xx}\frac{d\delta\phi}{dx} + \tau_{xy}\delta\phi\right) + \tau_{xy}\frac{d\delta w}{dx} + \left(\sigma_{yy}\delta\psi + y\tau_{xy}\frac{d\delta\psi}{dx}\right) \right. \\ &\quad \left. + \left(2y\sigma_{yy}\delta\beta + y^2\tau_{xy}\frac{d\delta\beta}{dx}\right) \right] dAdx. \end{aligned} \quad (5)$$

Introducing the stress resultants,

$$\begin{aligned} M &= \int_A y\sigma_{xx}dA, \quad N = \int_A \sigma_{xx}dA, \quad V = \int_A \tau_{xy}dA, \\ J &= \int_A y\tau_{xy}dA, \quad H = \int_A \sigma_{yy}dA, \quad S = \int_A y\sigma_{yy}dA, \\ T &= \int_A y^2\tau_{xy}dA, \end{aligned} \quad (6)$$

allows Eq. (5) to be written as

$$\begin{aligned} \delta U &= \int_{x_1}^{x_2} \left[N\frac{d\delta u}{dx} + \left(M\frac{d\delta\phi}{dx} + V\delta\phi\right) + V\frac{d\delta w}{dx} + \left(H\delta\psi + J\frac{d\delta\psi}{dx}\right) \right. \\ &\quad \left. + \left(2S\delta\beta + T\frac{d\delta\beta}{dx}\right) \right] dx. \end{aligned} \quad (7)$$

Integrating Eq. (7) by parts, the expression of the virtual strain energy becomes,

$$\begin{aligned} \delta U &= \int_{x_1}^{x_2} \left[-\frac{dN}{dx}\delta u + \left(V - \frac{dM}{dx}\right)\delta\phi - \frac{dV}{dx}\delta w + \left(H - \frac{dJ}{dx}\right)\delta\psi \right. \\ &\quad \left. + \left(2S - \frac{dT}{dx}\right)\delta\beta \right] dx + [N\delta u + M\delta\phi + V\delta w + J\delta\psi + T\delta\beta]_{x_1}^{x_2}. \end{aligned} \quad (8)$$

Next consider the axial and transverse distributed loads, $q_x^+(\theta)$, $q_x^-(\theta)$ and $q_y^+(\theta)$, $q_y^-(\theta)$, which are applied at the upper and lower lateral surfaces of the beam as illustrated in Fig. 1. The superscript “+” denotes quantities applied at the top surface and “−” denotes the quantities applied at the bottom surface. Using this notation along with the definitions in Eq. (1), the external virtual potential energy can be written as,

$$\begin{aligned} \delta V &= - \int_{x_1}^{x_2} \left[q_x^+ \delta u_x|_{y=\frac{h}{2}} + q_y^+ \delta u_y|_{y=\frac{h}{2}} + q_x^- \delta u_x|_{y=-\frac{h}{2}} + q_y^- \delta u_y|_{y=-\frac{h}{2}} \right] dx \\ &= - \int_{x_1}^{x_2} \left[(q_x^+ + q_x^-)\delta u + (q_y^+ + q_y^-)\delta w + (q_x^+ - q_x^-)\frac{h}{2}\delta\phi \right. \\ &\quad \left. + (q_y^+ - q_y^-)\frac{h}{2}\delta\psi \right] dx. \end{aligned} \quad (9)$$

The principle of virtual work states that the virtual work of a deformable continuum in equilibrium is zero, that is

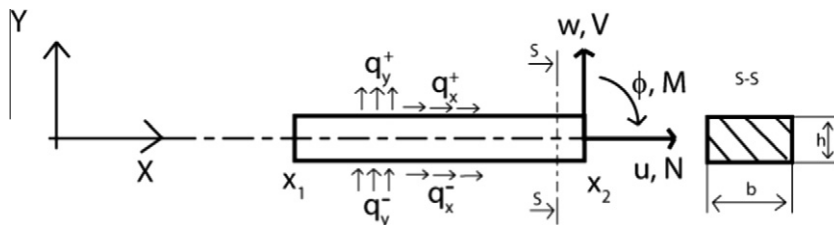


Fig. 1. One-dimensional model of a straight beam with surface tractions applied on the outer lateral surfaces.

$$\delta W = \delta U + \delta V = 0. \quad (10)$$

Combining Eqs. (8)–(10) gives,

$$\begin{aligned} \delta W = \int_{x_1}^{x_2} & \left[\left(-\frac{dN}{dx} - (q_x^+ + q_x^-) \right) \delta u + \left(V - \frac{dM}{dx} - \frac{h}{2}(q_x^+ - q_x^-) \right) \delta \phi \right. \\ & + \left(-\frac{dV}{dx} - (q_y^+ + q_y^-) \right) \delta w + \left(H - \frac{dJ}{dx} - \frac{h}{2}(q_y^+ - q_y^-) \right) \delta \psi \\ & + \left(2S - \frac{dT}{dx} - \frac{h^2}{4}(q_y^+ + q_y^-) \right) \delta \beta \Big] dx + [N\delta u + M\delta \phi + V\delta w \\ & + J\delta \psi + T\delta \beta]_{x_1}^{x_2} = 0. \end{aligned} \quad (11)$$

Eq. (11) is valid for any set of admissible virtual displacements. Thus, it follows that the static equilibrium equations of the beam are given by,

$$\begin{aligned} \frac{dN}{dx} &= -(q_x^+ + q_x^-), \\ V - \frac{dM}{dx} &= \frac{h}{2}(q_x^+ - q_x^-), \\ \frac{dV}{dx} &= -(q_y^+ + q_y^-), \\ H - \frac{dJ}{dx} &= \frac{h}{2}(q_y^+ - q_y^-), \\ 2S - \frac{dT}{dx} &= \frac{h^2}{4}(q_y^+ + q_y^-). \end{aligned} \quad (12)$$

These equilibrium equations are subject to the exclusive essential/natural boundary conditions given in Eq. (11).

2.1.2. Governing equations

Assuming conditions of plane stress for a linear orthotropic material with principal material directions coincident with the Cartesian coordinates,

$$\begin{bmatrix} \epsilon_{xx} \\ \epsilon_{yy} \\ \gamma_{xy} \end{bmatrix} = \begin{bmatrix} 1/E_1 & -\nu_{12}/E_2 & 0 \\ -\nu_{21}/E_1 & 1/E_2 & 0 \\ 0 & 0 & 1/G_{12} \end{bmatrix} \begin{bmatrix} \sigma_{xx} \\ \sigma_{yy} \\ \tau_{xy} \end{bmatrix}, \quad (13)$$

where $\nu_{12}E_1 = \nu_{21}E_2$; E_1, E_2 are the Young's moduli in the x and y directions, respectively; ν_{ij} is the Poisson's ratio that corresponds to the contraction in the i -direction when a traction is applied in the j -direction and $G = G_{12}$ is the transverse shear modulus.

Combining the material behavior relations, (13), with the strain-displacement relations, (3), allows the stress resultants, (6), to be expressed in terms of the displacement components,

$$\begin{aligned} M &= \int_A y \left[\frac{E_1}{1 - \nu_{12}\nu_{21}} \left(\frac{du}{dx} + y \frac{d\phi}{dx} \right) + \frac{\nu_{12}E_1}{1 - \nu_{12}\nu_{21}} (\psi + 2y\beta) \right] dA \\ &= \frac{EI_1}{1 - \nu_{12}\nu_{21}} \frac{d\phi}{dx} + \frac{2\nu_{12}EI_1}{1 - \nu_{12}\nu_{21}} \beta, \\ N &= \int_A \left[\frac{E_1}{1 - \nu_{12}\nu_{21}} \left(\frac{du}{dx} + y \frac{d\phi}{dx} \right) + \frac{\nu_{12}E_1}{1 - \nu_{12}\nu_{21}} (\psi + 2y\beta) \right] dA \\ &= \frac{EA_1}{1 - \nu_{12}\nu_{21}} \frac{du}{dx} + \frac{\nu_{12}EA_1}{1 - \nu_{12}\nu_{21}} \psi, \\ V &= \int_A G \left(\phi + \frac{dw}{dx} + y \frac{d\psi}{dx} + y^2 \frac{d\beta}{dx} \right) dA \\ &= GA \left(\phi + \frac{dw}{dx} \right) + GI \frac{d\beta}{dx}, \\ J &= \int_A yG \left(\phi + \frac{dw}{dx} + y \frac{d\psi}{dx} + y^2 \frac{d\beta}{dx} \right) dA = GI \frac{d\psi}{dx}, \\ H &= \int_A \left[\frac{E_2}{1 - \nu_{12}\nu_{21}} (\psi + 2y\beta) + \frac{\nu_{21}E_2}{1 - \nu_{12}\nu_{21}} \left(\frac{du}{dx} + y \frac{d\phi}{dx} \right) \right] dA \\ &= \frac{EA_2}{1 - \nu_{12}\nu_{21}} \psi + \frac{\nu_{21}EA_2}{1 - \nu_{12}\nu_{21}} \frac{du}{dx}, \\ S &= \int_A y \left[\frac{E_2}{1 - \nu_{12}\nu_{21}} (\psi + 2y\beta) + \frac{\nu_{21}E_2}{1 - \nu_{12}\nu_{21}} \left(\frac{du}{dx} + y \frac{d\phi}{dx} \right) \right] dA \\ &= \frac{2EI_2}{1 - \nu_{12}\nu_{21}} \beta + \frac{\nu_{21}EI_2}{1 - \nu_{12}\nu_{21}} \frac{d\phi}{dx}, \\ T &= \int_A y^2 G \left(\phi + \frac{dw}{dx} + y \frac{d\psi}{dx} + y^2 \frac{d\beta}{dx} \right) dA = GI \left(\phi + \frac{dw}{dx} \right) + GI \frac{d\beta}{dx}, \end{aligned} \quad (14)$$

where the six stiffness parameters introduced in the above equations are

$$\begin{aligned} EA_i &= \int_A E_i dA, \quad i = 1, 2, \quad EI_i = \int_A y^2 E_i dA, \quad i = 1, 2, \\ GA &= \int_A G dA, \quad GI = \int_A y^2 G dA, \quad GII = \int_A y^4 G dA. \end{aligned} \quad (15)$$

Substituting (14) into (12) gives the coupled unidirectional governing differential equations for the displacement field,

$$\begin{aligned} \frac{EA_1}{1 - \nu_{12}\nu_{21}} \frac{d^2 u}{dx^2} + \frac{\nu_{12}EA_1}{1 - \nu_{12}\nu_{21}} \frac{d\psi}{dx} &= -(q_x^+ + q_x^-), \\ -\frac{EI_1}{1 - \nu_{12}\nu_{21}} \frac{d^2 \phi}{dx^2} + GA\phi + GA \frac{dw}{dx} + \left(GI - \frac{2\nu_{12}EI_1}{1 - \nu_{12}\nu_{21}} \right) \frac{d\beta}{dx} &= \frac{h}{2}(q_x^+ - q_x^-), \\ GA \frac{d\phi}{dx} + GA \frac{d^2 w}{dx^2} + GI \frac{d^2 \beta}{dx^2} &= -(q_y^+ + q_y^-), \\ \frac{EA_2}{1 - \nu_{12}\nu_{21}} \psi - GI \frac{d^2 \psi}{dx^2} + \frac{\nu_{21}EA_2}{1 - \nu_{12}\nu_{21}} \frac{du}{dx} &= \frac{h}{2}(q_y^+ - q_y^-), \\ -GI \frac{d^2 \beta}{dx^2} + \frac{4EI_2}{1 - \nu_{12}\nu_{21}} \beta + \frac{2\nu_{21}EI_2}{1 - \nu_{12}\nu_{21}} \frac{d\phi}{dx} - GI \left(\frac{d\phi}{dx} + \frac{d^2 w}{dx^2} \right) &= \frac{h^2}{4}(q_y^+ + q_y^-). \end{aligned} \quad (16)$$

The above equations are the governing equations of a straight extensional transverse compliant beam within linear elasticity theory using the assumed displacement fields given by Eq. (1). The governing equations are subject to the following exclusive essential/natural boundary conditions,

$$\begin{aligned} w(x_i)/V(x_i) &= GA \left(\frac{dw}{dx} + \phi \right) + GI \frac{d\beta}{dx} \Big|_{x_i}, \\ u(x_i)/N(x_i) &= \frac{EA_1}{1 - \nu_{12}\nu_{21}} \frac{du}{dx} + \frac{\nu_{12}EA_1}{1 - \nu_{12}\nu_{21}} \psi \Big|_{x_i}, \\ \phi(x_i)/M(x_i) &= \frac{EI_1}{1 - \nu_{12}\nu_{21}} \frac{d\phi}{dx} + \frac{2\nu_{12}EI_1}{1 - \nu_{12}\nu_{21}} \beta \Big|_{x_i}, \\ \psi(x_i)/J(x_i) &= GI \frac{d\psi}{dx} \Big|_{x_i}, \\ \beta(x_i)/T(x_i) &= GI \left(\phi + \frac{dw}{dx} \right) + GI \frac{d\beta}{dx}; \quad i = 1, 2. \end{aligned} \quad (17)$$

When pressure is not applied to the outer lateral surfaces of the beam, the coupling between surface traction and transverse normal strain is negligible and the transverse normal strain is essentially zero along the x -axis. However, in contact problems the non-zero pressure quantity $h/2(q_y^+ - q_y^-)$ causes the normal transverse deformation to play a role. In order to help quantify this role, in the next two sections, formulations are presented for linear and constant transverse displacement, the latter case being the Timoshenko beam theory. In the results section, solutions for all three theories will be compared.

2.2. Linear beam theory

The formulation for the case of the linear beam theory is identical to that of the quadratic theory presented in Section 2.1, with the simplification that the function, $\beta(x)$ in (1)₂ is identically zero. As such, the assumed displacement field is given by

$$\begin{aligned} u_x(x, y) &= u(x) + y\phi(x), \\ u_y(x, y) &= w(x) + y\psi(x). \end{aligned} \quad (18)$$

The formulation from Eqs. (2)–(17) is valid for this case with $\beta(x) = 0$. Furthermore, the stress resultants, S and T , which are respectively associated with variations of β and its derivative in (7), are unnecessary to define. The stiffness parameters, EL_2 and GII in (15) are also unnecessary. The virtual work expression, analogous to Eq. (11) for the quadratic case, is therefore given by

$$\begin{aligned} \delta W = \int_{x_1}^{x_2} & \left[\left(-\frac{dN}{dx} - (q_x^+ + q_x^-) \right) \delta u + \left(V - \frac{dM}{dx} - \frac{h}{2} (q_x^+ - q_x^-) \right) \delta \phi \right. \\ & + \left(-\frac{dV}{dx} - (q_y^+ + q_y^-) \right) \delta w + \left(H - \frac{dJ}{dx} - \frac{h}{2} (q_y^+ - q_y^-) \right) \delta \psi \Big] dx \\ & + [N\delta u + M\delta \phi + V\delta w + J\delta \psi]_{x_1}^{x_2} = 0. \end{aligned} \quad (19)$$

From this expression it is seen that (12)₅, (16)₅, and the associated boundary conditions are not applicable to the linear case. Therefore, the governing equations reduce to

$$\begin{aligned} \frac{EA_1}{1 - \nu_{12}\nu_{21}} \frac{d^2 u}{dx^2} + \frac{\nu_{12}EA_1}{1 - \nu_{12}\nu_{21}} \frac{d\psi}{dx} &= -(q_x^+ + q_x^-), \\ -\frac{EI_1}{1 - \nu_{12}\nu_{21}} \frac{d^2 \phi}{dx^2} + GA\phi + GA \frac{dw}{dx} &= \frac{h}{2} (q_x^+ - q_x^-), \\ GA \frac{d\phi}{dx} + GA \frac{d^2 w}{dx^2} &= -(q_y^+ + q_y^-), \\ \frac{EA_2}{1 - \nu_{12}\nu_{21}} \psi + \frac{\nu_{21}EA_2}{1 - \nu_{12}\nu_{21}} \frac{du}{dx} - GI \frac{d^2 \psi}{dx^2} &= \frac{h}{2} (q_y^+ - q_y^-), \end{aligned} \quad (20)$$

which are subjected to the following exclusive essential/natural boundary conditions,

$$\begin{aligned} w(x_i)/V(x_i) &= GA \left(\frac{dw}{dx} + \phi \right) \Big|_{x_i}, \quad u(x_i)/N(x_i) = \frac{EA_1}{1 - \nu_{12}\nu_{21}} \frac{du}{dx} + \frac{\nu_{12}EA_1}{1 - \nu_{12}\nu_{21}} \psi \Big|_{x_i}, \\ \phi(x_i)/M(x_i) &= \frac{EI_1}{1 - \nu_{12}\nu_{21}} \frac{d\phi}{dx} \Big|_{x_i}, \quad \psi(x_i)/J(x_i) = GI \frac{d\psi}{dx} \Big|_{x_i}; \quad i = 1, 2. \end{aligned} \quad (21)$$

For the complete derivation for linear beam theory, the reader is referred to Gasmı (2011).

2.3. Timoshenko beam theory

Consider a Timoshenko displacement approximation with axial extension as follows,

$$\begin{aligned} u_x(x, y) &= u(x) + y\phi(x), \\ u_y(x, y) &= w(x) \end{aligned} \quad (22)$$

In terms of the quadratic formulation presented in Eqs. (1)–(17), this formulation cannot be presented as efficiently as that of the linear case. The portion of the formulation from Eqs. (2)–(8) is valid using $\psi(x) = 0$ and $\beta(x) = 0$. In Timoshenko beam theory, because of (22)₂, only the effects of σ_{xx} and τ_{xy} are accounted for, so only the stress resultants M , N and V are required. The expression for the virtual strain energy, which is analogous to (8), is given by

$$\begin{aligned} \delta U = \int_{x_1}^{x_2} & \left(-\frac{dN}{dx} \delta u + \left(-\frac{dM}{dx} + V \right) \delta \phi - \frac{dV}{dx} \delta w \right) dx + [N\delta u \\ & + M\delta \phi + V\delta w]_{x_1}^{x_2} \end{aligned} \quad (23)$$

Next, contrary to the linear and quadratic formulations, the transverse and circumferential distributed loads $q_x(x)$, $q_y(x)$, using Timoshenko beam theory, are applied at the centroidal axis of the beam as illustrated in Fig. 2. For this loading the external virtual potential energy can be written as,

$$\delta V = - \int_{x_1}^{x_2} (q_x \delta u + q_y \delta w) dx. \quad (24)$$

Applying the principle of virtual work, (10), gives

$$\begin{aligned} \delta W = \int_{x_1}^{x_2} & \left(\left(-\frac{dN}{dx} - q_x \right) \delta u + \left(-\frac{dM}{dx} + V \right) \delta \phi + \left(-\frac{dV}{dx} - q_y \right) \delta w \right) dx \\ & + [N\delta u + M\delta \phi + V\delta w]_{x_1}^{x_2} = 0, \end{aligned} \quad (25)$$

which leads to the equilibrium equations

$$\begin{aligned} \frac{dN}{dx} + q_x &= 0, \\ -\frac{dM}{dx} + V &= 0, \\ \frac{dV}{dx} + q_y &= 0, \end{aligned} \quad (26)$$

which are subjected to the exclusive essential/natural boundary conditions given in Eq. (25).

Similarly, following the steps presented in Eqs. (13)–(17) for the quadratic theory, the governing equations for extensional Timoshenko beam theory can be determined to be,

$$\begin{aligned} EA_1 \frac{d^2 u}{dx^2} + q_x &= 0, \\ -EI_1 \frac{d^2 \phi}{dx^2} + GA\phi + GA \frac{dw}{dx} &= 0, \\ GA \frac{d^2 w}{dx^2} + GA \frac{d\phi}{dx} + q_y &= 0, \end{aligned} \quad (27)$$

which are subjected to the following exclusive essential/natural boundary conditions,

$$\begin{aligned} w(x_i)/V(x_i) &= \frac{GA}{R} \left(\frac{dw}{dx} + \phi \right) \Big|_{x_i}, \quad u(x_i)/N(x_i) = EA_1 \frac{du}{dx} \Big|_{x_i}, \\ \phi(x_i)/M(x_i) &= EI_1 \frac{d\phi}{dx} \Big|_{x_i}; \quad i = 1, 2. \end{aligned} \quad (28)$$

The complete derivation of this case is given by Gasmı (2011).

3. Example – straight beam on a rigid smooth circular surface

The problem of a straight beam pressed onto a circular surface, as presented in Fig. 3, is interesting for two reasons. First, it is similar to the flattening of a circular beam, and second, it corresponds to constant curvature, and therefore constant bending moment using Euler-Bernoulli beam theory. Constant bending moment can only be achieved by point loads at the edge of contact. A slight modification of this theory for this geometry will induce a non-zero contact pressure.

When the beam is pressed on a rigid circular surface, two regions develop as illustrated in Fig. 3. These regions are the contact region, where the beam is supported by distributed contact stresses, and the free surface region, where distributed surface traction forces are zero. In the next sections, analytical solutions for each region are presented for the three beam theories. For simplicity, the in-plane Poisson's effect is neglected by setting $\nu_{12} = 0$ and $\nu_{21} = 0$, which for frictionless contact, decouples the axial displacement, u , from the contact pressure, q_y^- , as seen from Eq. (16). This Poisson effect, which is small, will be quantified later.

3.1. Free surface solution

In this region of the beam all distributed loads are zero. The solution to the governing equations, which is the homogenous solution, is obtained readily by decoupling the governing differential equations.

3.1.1. Timoshenko beam theory

In the case of Timoshenko theory, the solution to the governing equations given by Eq. (27) is as follows,

$$\begin{aligned} w(x) &= C_1 \frac{x^3}{6} + C_2 \frac{x^2}{2} + C_3 x + c_4, \quad \phi(x) = -C_1 \left(\frac{EI}{GA} + \frac{x^2}{2} \right) - C_2 x - C_3, \\ V(x) &= -EIC_1, \quad M(x) = -EIC_1 x - EIC_2 \end{aligned} \quad (29)$$

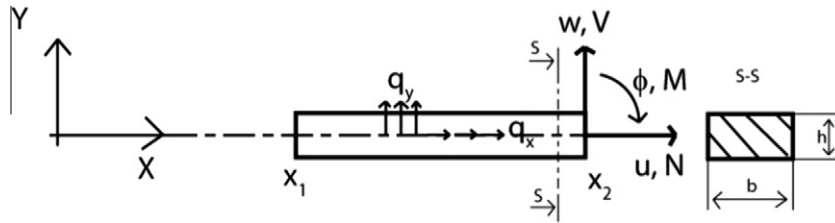


Fig. 2. One-dimensional model of a straight beam with surface tractions applied on the mid surface along x -axis.

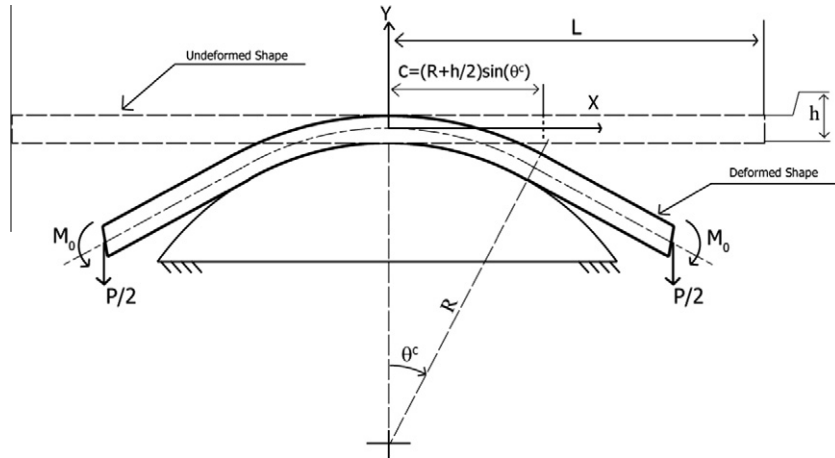


Fig. 3. A straight orthotropic beam in contact with a rigid smooth circular surface.

3.1.2. Linear beam theory

In the case of the linear beam theory, the solution to the governing equations given by Eq. (20)₂₋₄ with $\beta(x) = 0$ is as follows,

$$\begin{aligned} w(x) &= C_1 \frac{x^3}{6} + C_2 \frac{x^2}{2} + C_3 x + C_4, \\ \phi(x) &= -C_1 \left(\frac{EI}{GA} + \frac{x^2}{2} \right) - C_2 x - C_3, \\ \psi(x) &= C_5 \operatorname{ch} \left(x \sqrt{\frac{EA_2}{GI}} \right) + C_6 \operatorname{sh} \left(x \sqrt{\frac{EA_2}{GI}} \right), \\ V(x) &= -EIC_1, \quad M(x) = -EIC_1 x - EIC_2, \\ J(x) &= \sqrt{EA_2 GI} \left[C_5 \operatorname{sh} \left(x \sqrt{\frac{EA_2}{GI}} \right) + C_6 \operatorname{ch} \left(x \sqrt{\frac{EA_2}{GI}} \right) \right]. \end{aligned} \quad (30)$$

3.1.3. Quadratic beam theory

In the case of quadratic approximate beam theory, the solution to the governing equations given by Eq. (16)₂₋₅ is as follows,

$$\begin{aligned} w(x) &= C_1 - \frac{GI}{GA} [C_2 \exp(a_1 x) + C_3 \exp(-a_1 x)] - C_6 x - C_7 \frac{x^2}{2EI_1} \\ &\quad + C_8 \left(\frac{x}{GA} - \frac{x^3}{6EI_1} \right), \quad \phi(x) = C_6 + C_7 \frac{x}{EI_1} + C_8 \frac{x^2}{2EI_1}, \\ \psi(x) &= \frac{1}{\sqrt{EA_2 GI}} \left[C_4 \exp \left(x \sqrt{\frac{EA_2}{GI}} \right) - C_5 \exp \left(-x \sqrt{\frac{EA_2}{GI}} \right) \right], \\ \beta(x) &= C_2 \exp(a_1 x) + C_3 \exp(-a_1 x), \\ V(x) &= C_8, \quad M(x) = C_7 + C_8 x, \\ J(x) &= C_4 \exp \left(x \sqrt{\frac{EA_2}{GI}} \right) + C_5 \exp \left(-x \sqrt{\frac{EA_2}{GI}} \right), \\ T(x) &= \frac{4EI_2}{a_1} [C_2 \exp(a_1 x) - C_3 \exp(-a_1 x)] + C_8 \frac{GI}{GA}, \end{aligned} \quad (31)$$

where the constant introduced above is defined as

$$a_1 = 2 \sqrt{\frac{EI_2 GA}{GAGI - GI^2}}. \quad (32)$$

3.2. Contact solution

For the frictionless contact problem shown in Fig. 3, the contact boundary constraint for a straight beam on a rigid circular surface of radius R can be determined to be

$$\begin{aligned} u_y \left(x, z = -\frac{h}{2} \right) &= -R(1 - \cos(\theta)) = -R \left(1 - \sqrt{1 - \left(\frac{x}{R} \right)^2} \right) \\ &= -\frac{x^2}{2R} + O \left(\left(\frac{x}{R} \right)^4 \right). \end{aligned} \quad (33)$$

For small perturbation assumptions, the contact pressure is considered to be perpendicular to the initial surface of the beam, which is vertical.

3.2.1. Timoshenko beam theory

Using (33), the surface constraint for a Timoshenko theory is written as

$$w(x) = -\frac{x^2}{2R}. \quad (34)$$

Combined with the governing Eq. (27)₂₋₃, the solution of the symmetric contact problem is

$$\begin{aligned} q_y(x) &= -D_1 GA \sqrt{\frac{GA}{EI}} \operatorname{ch} \left(x \sqrt{\frac{GA}{EI}} \right), \quad w(x) = -\frac{x^2}{2R}, \\ \phi(x) &= D_1 \operatorname{sh} \left(x \sqrt{\frac{GA}{EI}} \right) + \frac{x}{r}, \\ V(x) &= D_1 GA \operatorname{sh} \left(x \sqrt{\frac{GA}{EI}} \right), \quad M(x) = D_1 \sqrt{EIGA} \operatorname{ch} \left(x \sqrt{\frac{GA}{EI}} \right) + \frac{EI}{R}. \end{aligned} \quad (35)$$

3.2.2. Linear beam theory

Using (33), the surface constraint for this case is written as follows,

$$w(x) - \frac{h}{2}\psi(x) = -\frac{x^2}{2R}. \quad (36)$$

Combined with the governing Eq. (20)₂₋₄, the uncoupled differential equation in contact pressure can easily be determined and its expression is given by,

$$\frac{d^4 q_y^-}{dx^4} + A \frac{d^2 q_y^-}{dx^2} + B q_y^- = 0, \quad (37)$$

where

$$A = -\frac{4(GAGI + EA_2 EI_1)}{EI_1(4GI + h^2 GA)}, \quad B = \frac{4GA EA_2}{EI_1(4GI + h^2 GA)}. \quad (38)$$

The solution for symmetric contact can then be determined to be,

$$\begin{aligned} q_y^-(x) &= D_1 \text{ch}(x\lambda_1) + D_2 \text{ch}(x\lambda_2), \\ w(x) &= -\frac{x^2}{2R} + \sum_{i=1}^2 \frac{h^2}{4(\lambda_i^2 GI - EA_2)} D_i \text{ch}(x\lambda_i), \\ \phi(x) &= \frac{x}{R} - \sum_{i=1}^2 \frac{1}{EI_1 \lambda_i^3} D_i \text{sh}(x\lambda_i), \quad \psi(x) = \sum_{i=1}^2 \frac{h}{2(\lambda_i^2 GI - EA_2)} D_i \text{ch}(x\lambda_i), \\ V(x) &= \sum_{i=1}^2 GA \frac{(4EA_2 - 4\lambda_i^2 GI + \lambda_i^2 h^2 EI_1)}{4EI_1 \lambda_i^3 (\lambda_i^2 GI - EA_2)} D_i \text{sh}(x\lambda_i), \\ M(x) &= \frac{EI_1}{R} - \sum_{i=1}^2 \frac{1}{\lambda_i^2} D_i \text{ch}(x\lambda_i), \\ J(x) &= \sum_{i=1}^2 \frac{h\lambda_i GI}{2(\lambda_i^2 GI - EA_2)} D_i \text{sh}(x\lambda_i), \end{aligned} \quad (39)$$

where

$$\lambda_1 = \frac{1}{2} \sqrt{-2A + 2\sqrt{A^2 - 4B}}, \quad \lambda_2 = \frac{1}{2} \sqrt{-2A - 2\sqrt{A^2 - 4B}}. \quad (40)$$

3.2.3. Quadratic beam theory

Using (33), the surface constraint for this case is written as follows,

$$w(x) - \frac{h}{2}\psi(x) + \frac{h^2}{4}\beta(x) = -\frac{x^2}{2R}. \quad (41)$$

Combined with the governing Eq. (16)₂₋₅, the uncoupled differential equation in contact pressure can readily be determined and its expression is given by,

$$\frac{d^6 q_y^-}{dx^6} + A \frac{d^4 q_y^-}{dx^4} + B \frac{d^2 q_y^-}{dx^2} + C q_y^- = 0, \quad (42)$$

where the coefficients in (42) are given by

$$\begin{aligned} A &= -\frac{16EI_1 EA_2 GII - 8EI_1 GIEA_2 h^2 + EI_1 GAh^4 EA_2 + 16GII GAGI}{EI_1(-12GI^2 h^2 + 4GII GAh^2 + GIGA h^4 + 16GII GI)} \\ &\quad - \frac{64EI_1 GIEI_2 - 16GI^3 + 16EI_1 EI_2 GAh^2}{EI_1(-12GI^2 h^2 + 4GII GAh^2 + GIGA h^4 + 16GII GI)}, \\ B &= 16 \frac{-GI^2 EA_2 + 4EA_2 EI_2 EI_1 + 4GA EI_2 GI + GAGII EA_2}{EI_1(-12GI^2 h^2 + 4GII GAh^2 + GIGA h^4 + 16GII GI)}, \\ C &= \frac{-64GA EA_2 EI_2}{EI_1(-12GI^2 h^2 + 4GII GAh^2 + GIGA h^4 + 16GII GI)}. \end{aligned} \quad (43)$$

Solution of the symmetric contact problem can be then determined to be,

$$\begin{aligned} q_y^-(x) &= D_1 \text{ch}(x\lambda_1) + D_2 \text{ch}(x\lambda_2) + D_3 \text{ch}(x\lambda_3), \\ w(x) &= -\frac{x^2}{2R} - \sum_{i=1}^3 a_{2i} D_i \text{ch}(x\lambda_i), \\ \phi(x) &= \frac{x}{R} - \sum_{i=1}^3 \frac{1}{EI_1 \lambda_i^3} D_i \text{sh}(x\lambda_i), \\ \psi(x) &= \sum_{i=1}^3 \frac{h}{2(\lambda_i^2 GI - EA_2)} D_i \text{ch}(x\lambda_i), \\ \beta(x) &= \sum_{i=1}^3 a_{3i} D_i \text{ch}(x\lambda_i), \quad V(x) = -\sum_{i=1}^3 \frac{1}{\lambda_i} D_i \text{sh}(x\lambda_i), \\ M(x) &= \frac{EI_1}{R} - \sum_{i=1}^3 \frac{1}{\lambda_i^2} D_i \text{ch}(x\lambda_i), \\ J(x) &= \sum_{i=1}^3 \frac{h\lambda_i GI}{2(\lambda_i^2 GI - EA_2)} D_i \text{sh}(x\lambda_i), \\ T(x) &= \sum_{i=1}^3 \left[-GI a_{2i} \lambda_i - \frac{GI}{EI_1 \lambda_i^3} + GII a_{3i} \right] D_i \text{sh}(x\lambda_i), \end{aligned} \quad (44)$$

where the λ_i are square roots of the three distinct roots of the characteristic equation,

$$X^3 + AX^2 + BX + C = 0, \quad (45)$$

and the constants introduced in (44) are

$$\begin{aligned} a_{2i} &= \frac{h^2 (-4GAGII \lambda_i^2 - 4GIEA_2 + 8GI^2 \lambda_i^2 + 16GA EI_2 + GAh^2 EA_2 - GAh^2 GI \lambda_i^2)}{16(EA_2 - GI \lambda_i^2) (GI^2 \lambda_i^2 + 4GA EI_2 - GAGII \lambda_i^2)}, \\ a_{3i} &= \frac{(GAh^2 - 4GI) \lambda_i}{4(GI^2 \lambda_i^2 + 4GA EI_2 - GAGII \lambda_i^2)}. \end{aligned} \quad (46)$$

4. Solution of the contact problem

Resolving the problem of contact of a straight beam on a circular surface is accomplished through applying all boundary conditions at the end of the beam and matching the essential and natural quantities at the edge of the contact area. The location of the edge of the contact area, c , is an unknown, which is determined by matching the essential and natural quantities to satisfy continuity at the contact edge. For the case of Timoshenko beam theory, the solutions are easily written in closed form. However, for the linear and quadratic theories, a lengthy nonlinear transcendental equation that relates the contact length and boundary conditions, which are applied to the end of the beam, is obtained and solved numerically to obtain all the results. In addition, the associated expressions, which are obtained analytically, are too lengthy to provide.

4.1. Timoshenko beam theory

Following Fig. 3, the boundary conditions for the case of a Timoshenko beam are,

$$V(L) = -\frac{P}{2}, \quad M(L) = M_0. \quad (47)$$

Continuity conditions at the edge of the contact area are given by,

$$w^I(c) = w^{II}(c), \quad \phi^I(c) = \phi^{II}(c), \quad V^I(c) = V^{II}(c), \quad M^I(c) = M^{II}(c). \quad (48)$$

The total number of unknowns is six, which includes four unknown integration constants from the free surface region, one integration constant from the contact region, plus the half contact

length, c . Resolving the linear system of equations analytically for the integration constants using Eqs. (48) and (47)₂, the transcendental equation which relates the contact length and the total transverse load and bending moment is obtained from Eq. (47)₁ as follows,

$$P = 2 \frac{EI}{R} \left(1 - \frac{M_0 R}{EI} \right) \left\{ L - c + \sqrt{\frac{EI}{GA}} \coth \left[c \sqrt{\frac{GA}{EI}} \right] \right\}^{-1}. \quad (49)$$

The final expression of the contact pressure is obtained from (35)₁, and can be written as,

$$q_y = \left[\frac{EI}{R} - M_0 - \frac{P}{2}(L - c) \right] \frac{GA}{EI} \operatorname{ch} \left(x \sqrt{\frac{GA}{EI}} \right) \left[\operatorname{ch} \left(c \sqrt{\frac{GA}{EI}} \right) \right]^{-1}. \quad (50)$$

Substituting M_0 from (49) into (50) gives the expression of the pressure in terms of the total force,

$$q_y = \frac{P}{2} \sqrt{\frac{GA}{EI}} \operatorname{ch} \left(x \sqrt{\frac{GA}{EI}} \right) \left[\operatorname{sh} \left(c \sqrt{\frac{GA}{EI}} \right) \right]^{-1}. \quad (51)$$

4.2. Linear beam theory

The boundary conditions for the linear beam theory are,

$$V(L) = -\frac{P}{2}, \quad M(L) = M_0, \quad J(L) = J_0, \quad (52)$$

and the continuity conditions at the edge of the contact area are given by,

$$\begin{aligned} w^I(c) &= w^{II}(c), & \phi^I(c) &= \phi^{II}(c), & \psi^I(c) &= \psi^{II}(c), \\ V^I(c) &= V^{II}(c), & M^I(c) &= M^{II}(c), & J^I(c) &= J^{II}(c) \end{aligned} \quad (53)$$

The total number of unknowns is nine, which includes six unknown integration constants from the free surface region, two unknown integration constants from the contact region, plus the half contact length, c . The solution procedure was to resolve the linear system of equations analytically for the integration constants using Eqs. (53) and (52)₂₋₃ in terms of the half contact length. Then by using Eq. (52)₁, a transcendental equation was obtained that relates the contact length, the total transverse loading P , the bending moment M_0 , and the moment of shearing J_0 (52). This analytical expression, which is too lengthy to provide, is solved numerically. The eight integration constants are then known, which allows all the expression in (30) and (39) to be determined.

4.3. Quadratic beam theory

The boundary conditions for the case of quadratic approximate beam theory are,

$$V(L) = -\frac{P}{2}, \quad M(L) = M_0, \quad J(L) = J_0, \quad T(L) = T_0. \quad (54)$$

Continuity conditions at the end of contact area are given by,

$$\begin{aligned} w^I(c) &= w^{II}(c), & \phi^I(c) &= \phi^{II}(c), & \psi^I(c) &= \psi^{II}(c), & \beta^I(c) &= \beta^{II}(c) \\ V^I(c) &= V^{II}(c), & M^I(c) &= M^{II}(c), & J^I(c) &= J^{II}(c), & T^I(c) &= T^{II}(c) \end{aligned} \quad (55)$$

The total number of unknowns is 12, which includes eight unknown integration constants from the free surface region, three from the contact region, plus the half contact length, c . The solution procedure used here is similar to that used for the linear case. The first step is to resolve the linear system of equations analytically for the integration constants using Eqs. (55) and (54)₂₋₄. Then a

transcendental equation which relates the contact length, the total transverse loading P , the bending moment M_0 , the moment of shearing J_0 and T_0 can be obtained from Eq. (54)₁.

5. Results and discussion

All the forthcoming results are obtained by using the geometrical constraints, $R/L = 3$ and $h/L = 0.05$. These ratios were chosen so that the large deflection effects are minimized in the solutions. The boundary conditions that are used in all results are for $M_0 = 0$, $J_0 = 0$, $T_0 = 0$. The normalized contact length, c/h , is used as the input loading parameter in all beam theory results. In the case of the finite element solutions, the vertical displacement was used to achieve a certain contact length. Since the Poisson effect was neglected in the analytical solutions, it is also neglected for all the plane elasticity finite element results that are used for comparisons. Identical to the beam theory results, this is accomplished by using an orthotropic material with $\nu_{12} = \nu_{21} = 0$, and E_1 , E_2 and G used as independent material inputs. For example, an isotropic material defined by the standard constants, E and ν , is addressed by using the orthotropic material properties, $E_1 = E_2 = E$, $G = E/2(1 + \nu)$, $\nu_{12} = \nu_{21} = 0$.

5.1. Isotropic beam ($\nu = 0.3$)

Normalized pressure profiles for an isotropic beam are presented in Fig. 4(a) and (b). In Fig. 4(a) the in-plane Poisson effect is quantified by using two plane stress elasticity solutions, which were obtained using the finite element software, ABAQUS. One solution is the true plane stress solution for an isotropic material with $\nu = 0.3$, while the other is for an isotropic material using the set of orthotropic material constants, $E_1 = E_2$, $G = E_2/2(1 + 0.3)$, $\nu_{12} = \nu_{21} = 0$, which allows the in-plane Poisson effect to be neglected in an elasticity solution. It is observed that for the four cases of contact length presented, the significance of the in-plane Poisson effect is relatively small.

Normalized pressure solutions for all three beam theories are presented in Fig. 4(b), along with the elasticity solution that does not include the Poisson effect. Since the beam theories correspond to a zero value of the Poisson's ratio, the results of Fig. 4(b) show the true comparison between the beam theories and the elasticity solution. The figures show that the contact stress exhibits three trends based on the length of the contact area. When the half-contact length, c is smaller than the thickness, h of the beam, a Hertz-like contact stress is obtained which corresponds to a concave downward profile with a maximum contact pressure at the center of the contact area. As the half contact length is increased above the thickness, a Timoshenko beam behavior starts to emerge, where the contact pressure at the center is a minimum while the maximum pressure approaches the contact edge. Beyond a certain critical contact length, a negative pressure appears in the center of the contact region, indicating that adhesion is required to satisfy the contact boundary condition. The critical contact length is defined as the contact length at which the pressure at the center of the beam first becomes zero as load is increased. The critical contact lengths for the three beam theories are: Timoshenko theory, $c/h > 10$, linear theory, $c/h = 3.303$ and quadratic theory, $c/h = 3.045$. While negative pressure is non-physical in simple contact problems, the model is correct if adhesion is permitted. Lacking this adhesive capability, the model predicts that the beam deforms in such a way that a loss of contact occurs at the center with two contact zones. As this mechanism continues, high concentrated contact stresses can develop with a relatively large loss of contact in the middle. In the limiting case of Euler-Bernoulli beam behavior, concentrated forces exist at the edge of contact. To quantify the

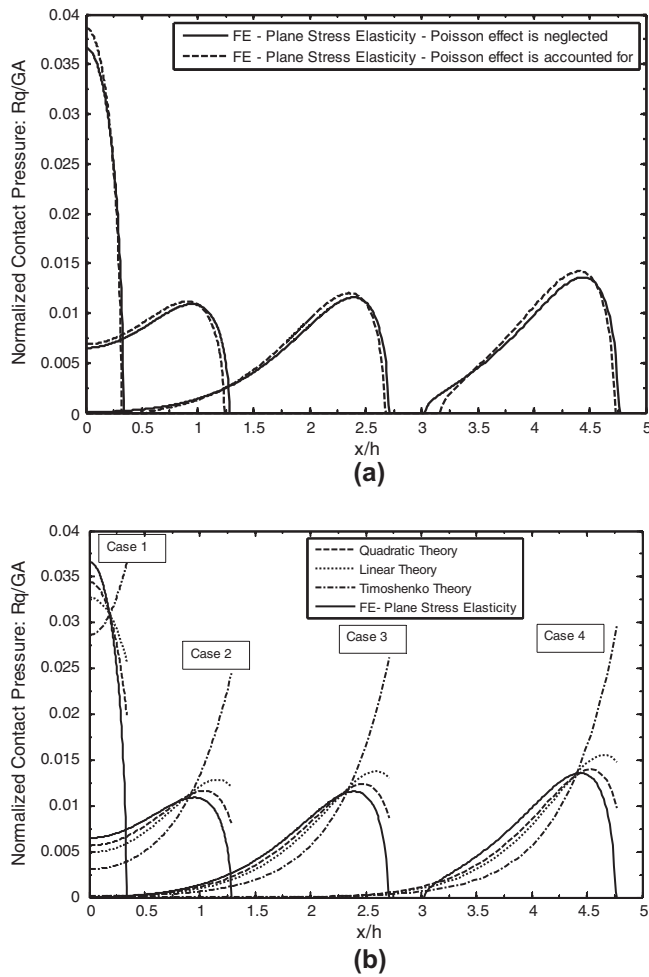


Fig. 4. Comparison of normalized contact stress solutions for an isotropic material ($\nu = 0.3$): (a) Plane elasticity solutions obtained from the finite element software Abaqus with and without the in-plane Poisson effect, (b) Present higher order theories, Timoshenko beam theory and plane stress elasticity all neglecting the in-plane Poisson effect.

Table 1

Total transverse load and contact length for the four different loading cases in Fig. 4a obtained for $E = 1 \text{ GPa}$, $b = 60 \text{ mm}$ and $L = 1$. The input loading corresponds to constant vertical displacement.

Case number	Deflection: $W(L)$ [mm]	c/h		Total transverse load [N]	
		Poisson effect is accounted for	Poisson effect is neglected	Poisson effect is accounted for	Poisson effect is neglected
1	100	0.323116	0.339708	374.246	374.084
2	112.5	1.24121	1.284934	421.858	421.748
3	120	2.67772	2.71278	456.278	456.154
4	130	4.73112	4.77164	518.096	517.914

effect of negative pressure in case 4 of Fig. 4(b), for the linear theory the ratio of the force associated with negative pressure to the total pressure force is 0.00032 and for the quadratic theory this ratio is 0.0010. Therefore, the pressure curves presented in case 4 of Fig. 4(b) are reasonable predictions of the pressure. Such a double contact problem was addressed by Chen (2011) using Timoshenko beam theory.

The most interesting behavior in Fig. 4b concerns the stress at the edge of contact. The Timoshenko solution, which neglects

Table 2

Total transverse load for the loading cases in Fig. 4b obtained for $E = 1 \text{ GPa}$, $b = 60 \text{ mm}$ and $L = 1 \text{ m}$.

Case number	c/h	Total transverse load [N]			
		FE- Plane stress elasticity theory	Quadratic theory	Linear theory	Timoshenko theory
1	0.339708	374.084	392.9946	398.8341	408.3465
2	1.284934	421.748	430.7728	431.7831	434.3834
3	2.71278	456.154	465.0868	466.302	469.4121
4	4.77164	517.914	525.4657	527.0174	530.9941

transverse normal deformation of the cross-section and only accounts for transverse shear and bending, presents a discrepancy in determining the value and location of the maximum contact stress. Moreover, the contact stress is discontinuous at the edge of the contact area. The solutions for the higher order theories, which account for transverse normal cross-sectional deformation, predict a better trend of the contact stress at the ends, yet are still discontinuous. Clearly the quadratic theory is an improvement on the linear theory, regarding this trend. Consequently, if the maximum contact stress is a design parameter, then the present higher order theories are a better substitute to the elasticity solution than the Timoshenko theory, which does not predict the correct trend of a decreasing contact stress at the edge of contact.

Furthermore, in comparison of the results of Fig. 4(a) which are for constant vertical displacement, it can be noticed that the Poisson's effect quickens the occurrence of contact separation at the center and slightly increases the maximum contact pressure. Since the results in Fig. 4(b) are for constant contact length and those of Fig. 4(a) have approximately the same contact length, it is important to consider the transverse total load. The values in Table 1 present the total transverse load required by the elasticity cases in Fig. 4(a), while Table 2 is the same for Fig. 4(b). As a general statement, since the beam theories have constraints compared to the elasticity solutions, the beam theories are stiffer and therefore require a higher load. The higher order the theory, the less the constraint so the load is closer to that of the elasticity result. By comparing the results in Tables 1 for the elasticity solution, Poisson's effect makes the beam slightly stiffer.

Finally, the inclusion of a shear correction factor (see, for example, Cowper (1966) and Hodges (2003)), such as a value of $5/6$ for the Timoshenko theory, changes the results very slightly compared to the differences among the different beam theory pressure profiles. The effects of shear correction factors, which are non-trivial to determine for the higher order beam theories, are not included in this study.

The results in Fig. 5 present the normalized displacement components and stress resultants obtained using both higher order theories and the Timoshenko beam theory. All results are obtained for a half contact length $c = 2h$. Even though contact pressure is very sensitive to the inclusion of transverse normal deformation, as shown in Fig. 4(a) and (b), the displacement components and stress resultants are affected very little. Furthermore, in Fig. 5(b), it can be seen from the bending moment curve that the normalized moment reaches a constant plateau in the contact region $RM/EI = 1$. Also an abrupt jump of the shearing force at the edge of contact can be observed. These later observations are consistent with the classical Euler-Bernoulli hypothesis on the normality of the cross-section to the neutral fiber after deformation for the case of a thin isotropic continuum strip.

The results in Fig. 6 compare the normalized total transverse load versus normalized contact length for the case of an isotropic material ($\nu = 0.3$) obtained by using both present higher order

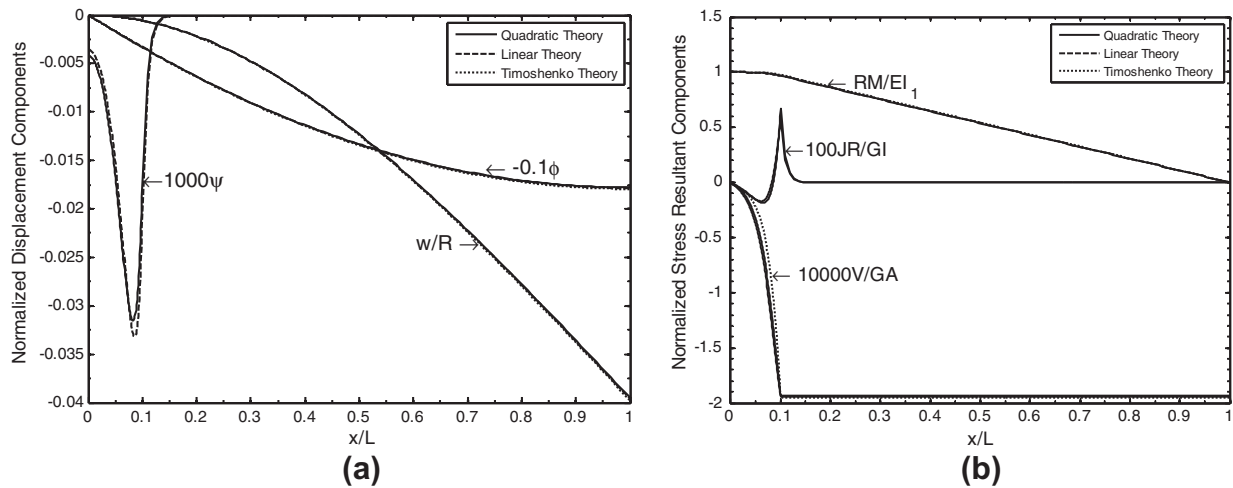


Fig. 5. Comparison of solutions from the present higher order theories and the Timoshenko theory for an isotropic material ($\nu = 0.3$) and contact length of $c = 2h$ (a) displacement components (b) stress resultants.

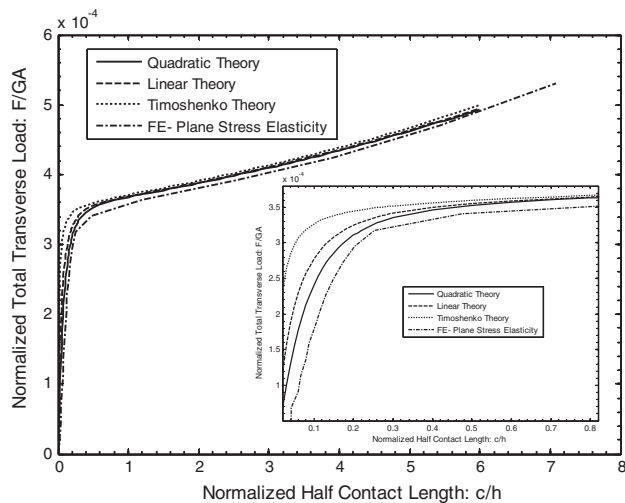


Fig. 6. Comparison of normalized total transverse load versus normalized contact length for an isotropic material ($\nu = 0.3$).

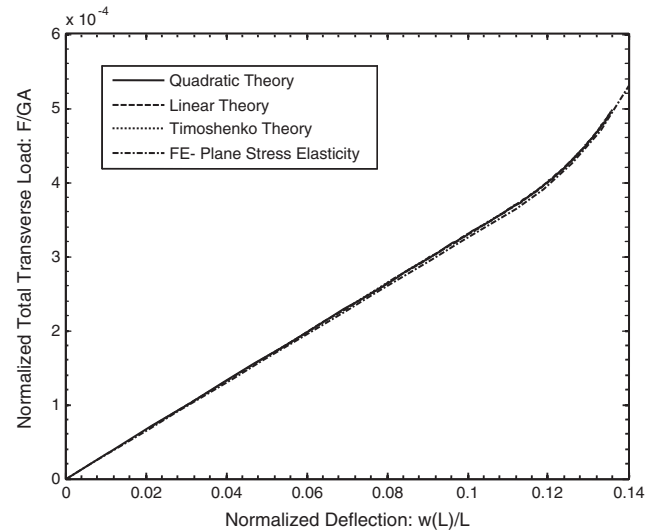


Fig. 7. Comparison of normalized total transverse load versus normalized deflection of the end of the beam for an isotropic material ($\nu = 0.3$).

beam theories, Timoshenko theory and plane stress elasticity theory. In all these solution, the in-plane Poisson's effect is neglected. All solutions obtained using beam theories overestimate the elasticity solution as it was discussed above. Furthermore, as expected, the quadratic theory solution is the closest to the elasticity solution and the Timoshenko one is the furthest.

Similar to the results of Fig. 6, the plots in Fig. 7 compare the normalized total transverse load versus normalized transverse deflection of the end of the beam in the case of an isotropic material ($\nu = 0.3$) for all the theories. All solutions in this case are in good agreement making the total transverse load vs. deflection response unaffected by neglecting transverse normal deformation in the case of a long isotropic beam. This result is consistent with Saint Venant's principle which states that the stress resultants should be unaffected by the local stress deviation to obtain same deflection.

5.2. Orthotropic beam I ($E_1/G = 10^4$, $E_2/G = 10$, $\nu_{12} = \nu_{21} = 0$)

In this section, the material properties are selected such that shear is the dominant mode of deformation. All results in this sec-

tion neglect the Poisson effect and correspond to the stiffness ratios, $E_1/G = 10^4$, $E_2/G = 10$. In composite science this material behavior can be obtained by means of sandwich or laminated composite construction. Such a "shearing band", which can have G and also E_2 much smaller than E_1 , was considered in detail by Gasmi et al. (2011) for the case of an extensional Timoshenko circular beam. See also Gasmi et al. (2012) for the practical application of a non-pneumatic tire that makes use of such beam construction.

The normalized contact stress results in Fig. 8 are for three different contact lengths, and once again are obtained using the present higher order theories, Timoshenko theory and plane stress elasticity theory. The graph shows that the Timoshenko solution and the two other higher order overlap everywhere in the contact area except at the edge of contact. However, the Timoshenko solution is maximum and discontinuous at the edge of contact while both higher order solutions exhibit a tendency to decrease, yet are still discontinuous. It is clear that including the normal deformation enhances the contact stress solution by giving the correct trend of pressure at the edge of the contact area even though it still provides a finite value. Moreover, both Timoshenko and the higher

order theories exhibit a slight gap with the elasticity. This discrepancy can only be resolved by including more monomials in the expressions of the displacement field, i.e. warping, or by using a shear correction factor. Again, as demonstrated in Table 2, the beam theories are stiffer than the elasticity solution.

The results in Fig. 9 compare the total force versus the contact length obtained by the present higher order theories, Timoshenko theory and the plane stress elasticity theory. All curves follow the same trend with an increasing gap between the beam theories and the elasticity solution as the contact length increases. The insert in the figure shows that force versus contact length presents a hardening behavior at small contact lengths, which is only captured by the present higher order theories. This shows that including radial deformation is crucial to determine this feature.

The results in Fig. 10 compare the total force versus deflection curve obtained by the present higher order theories, Timoshenko theory and the plane stress elasticity theory. From the figure it can be noticed that all beam theory solutions overlap and overshoot the elasticity solution. Although all solutions exhibit the same trend, the gap increases as the deflection is increased.

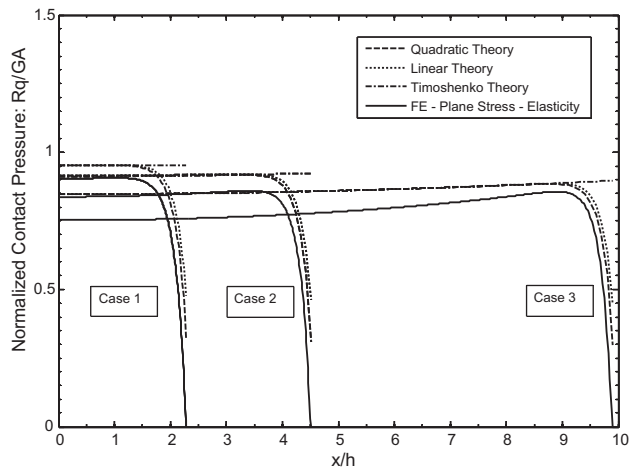


Fig. 8. Comparison of normalized contact stress in the case of orthotropic material I ($E_1/G = 10^4$, $E_2/G = 10$, $\nu_{12} = \nu_{21} = 0$) using the present higher order theories, Timoshenko theory and plane stress elasticity neglecting the Poisson effect.

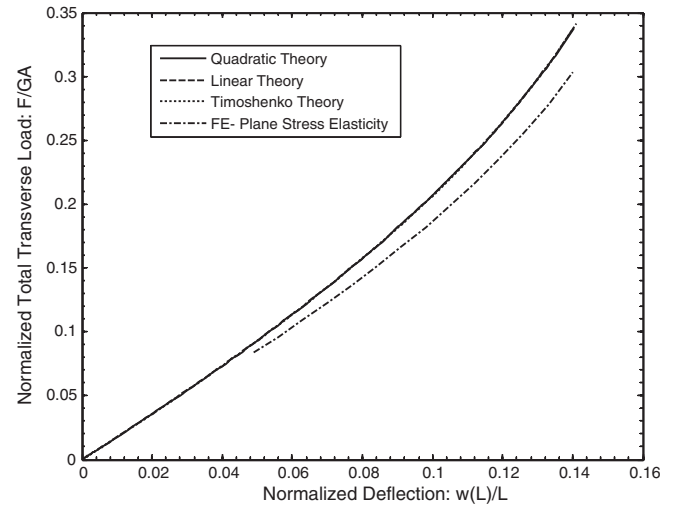


Fig. 10. Comparison of normalized total transverse load as a function of normalized deflection of the end of the beam for orthotropic material I defined in Fig. 8.

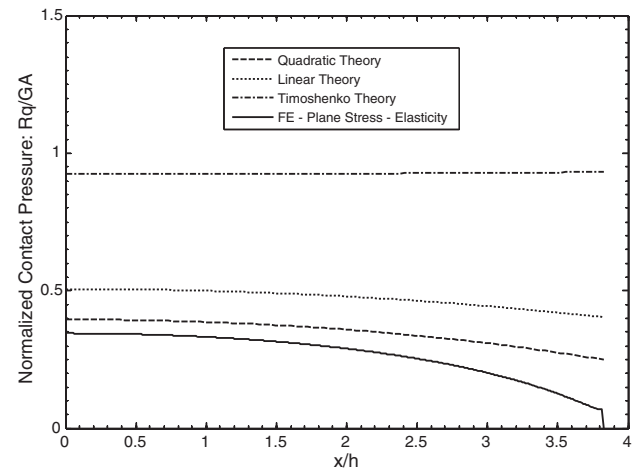


Fig. 11. Comparison of normalized contact stress in the case of orthotropic material II ($E_1/G = 10^4$, $E_2/G = 10^{-2}$, $\nu_{12} = \nu_{21} = 0$) using the present higher order theories, Timoshenko theory and plane stress elasticity neglecting the Poisson effect.

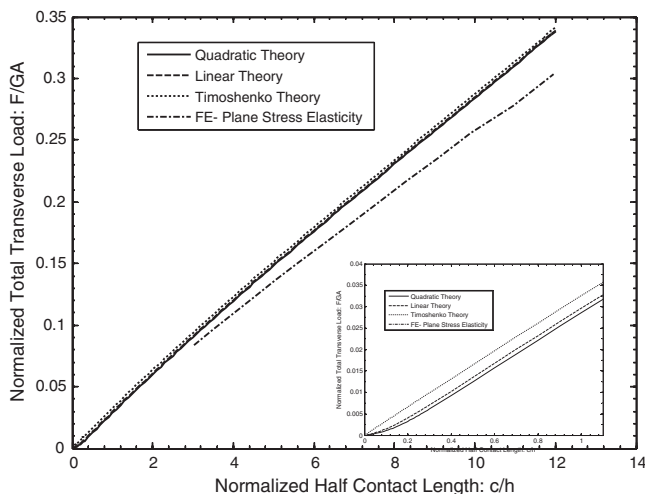


Fig. 9. Comparison of normalized total transverse load as a function of normalized contact length for orthotropic material I defined in Fig. 8.

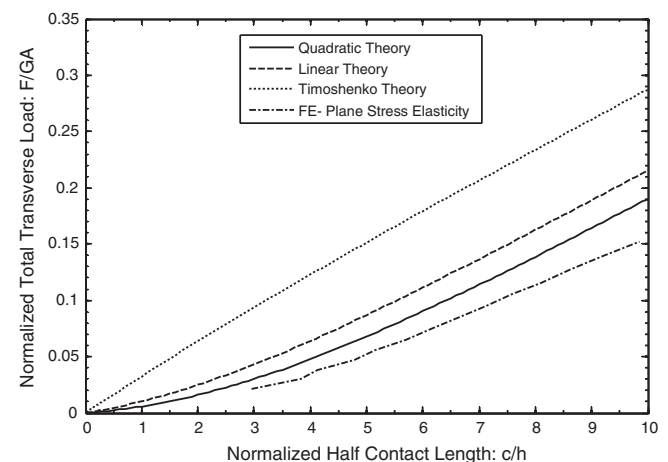


Fig. 12. Comparison of normalized total transverse load as a function of normalized contact length for orthotropic material II defined in Fig. 11.

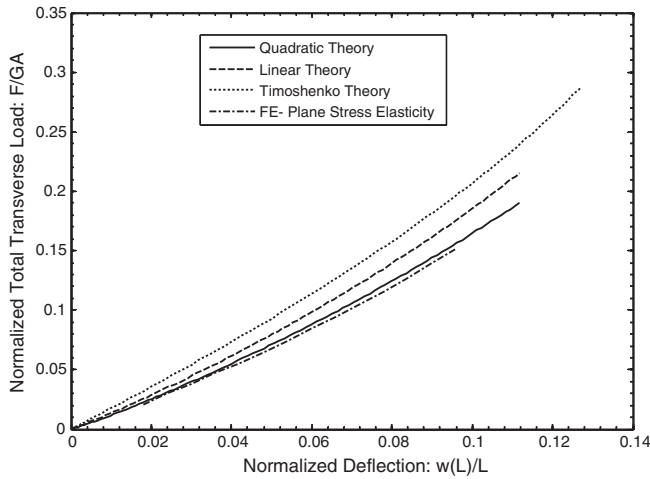


Fig. 13. Comparison of normalized total transverse load as a function of normalized deflection of the end of the beam for orthotropic material II defined in Fig. 11.

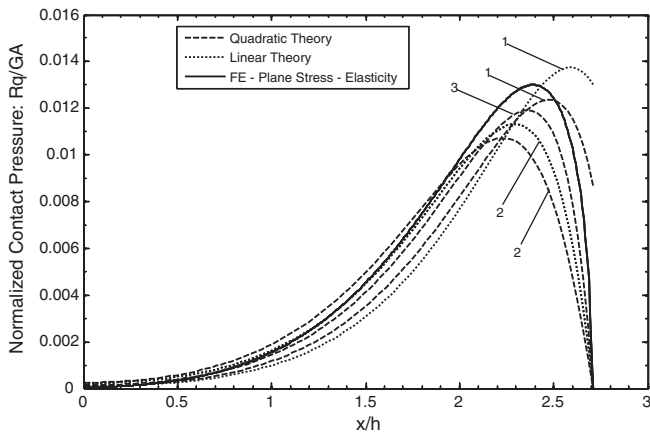


Fig. 14. Comparison of normalized contact stress for an isotropic material ($\nu = 0.3$) using the present higher order theories, Timoshenko theory and plane stress elasticity solution obtained using the finite element software Abaqus with the Poisson effect neglected. The following three cases are considered: (1) consistent boundary conditions, (2) continuity of ψ is violated and continuity of contact stress is enforced and (3) continuity of β is violated and continuity of contact stress is enforced.

5.3. Orthotropic beam II ($E_1/G = 10^4$, $E_2/G = 10^{-2}$, $\nu_{12} = \nu_{21} = 0$)

In this section the stiffness parameters are given by $E_1/G = 10^4$, $E_2/G = 10^{-2}$, which corresponds to the shearing band of the previous section with a much softer radial stiffness.

The results in Fig. 11 show a comparison of the normalized contact pressure obtained by the beam theories and by elasticity theory for the same contact length. It can be noticed that Timoshenko beam theory fails to estimate the contact pressure when a transverse normal compliance is added while the higher order beam theories, which include the transverse normal cross-sectional deformation, are much closer to the elasticity one. Furthermore, the quadratic beam theory is much closer than the linear one to the elasticity solution because of the importance of transverse normal deformation of the cross-section in this special case. In order to improve the beam theory results, it is necessary to include more detail of the axial component of the displacement vector, i.e. warping of the cross-section.

Furthermore, because all these approximate beam theories are constrained theories of the more general theory, i.e. elasticity theory, the contact pressure is overestimated and the total load is larger than the elasticity one for the same deflection making the approximate theories stiffer.

The results in Fig. 12 present the total load as a function of contact length for all the theories. Once again, it can be seen that the quadratic is the closest to the elasticity result and that both higher order beam theories are significantly better than the Timoshenko beam, making the inclusion of transverse normal deformation in this special case critical to the determination of an accurate solution to the problem.

The results in Fig. 13 show the total load as a function of the deflection at the end of the beam for the different solutions of the beam theories and the elasticity theory. Once again, the figure proves that the quadratic theory is the closest to the elasticity solution and therefore the inclusion of the transverse normal deformation is required for the accurate determination of the solution to this special case.

5.4. Pressure at the edge of contact

In this section the contact pressure as predicted by the higher order beam theories is forced to drop to zero at the edge of contact. Such behavior is required in linear elasticity for contact involving

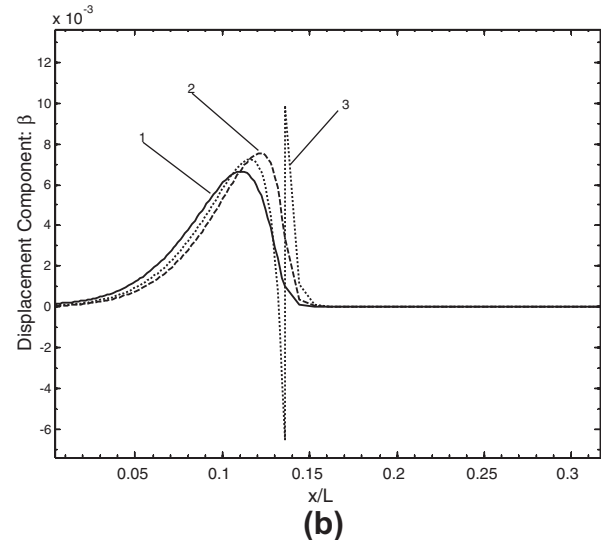
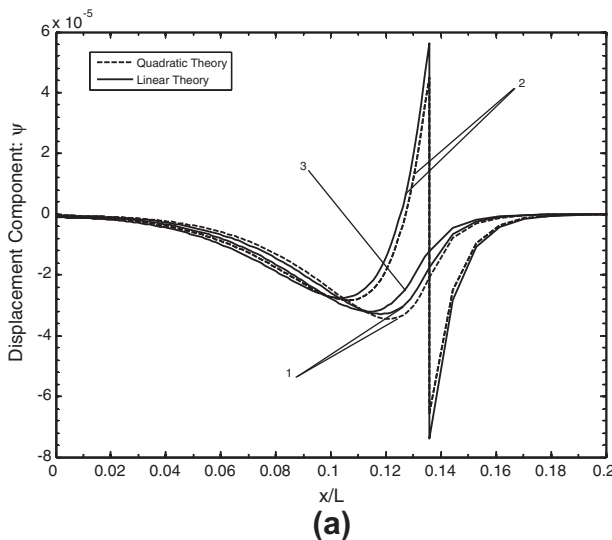


Fig. 15. Continuity study of the displacement components, ψ and β , for the five cases in Fig. 14: (a) ψ , (b) β .

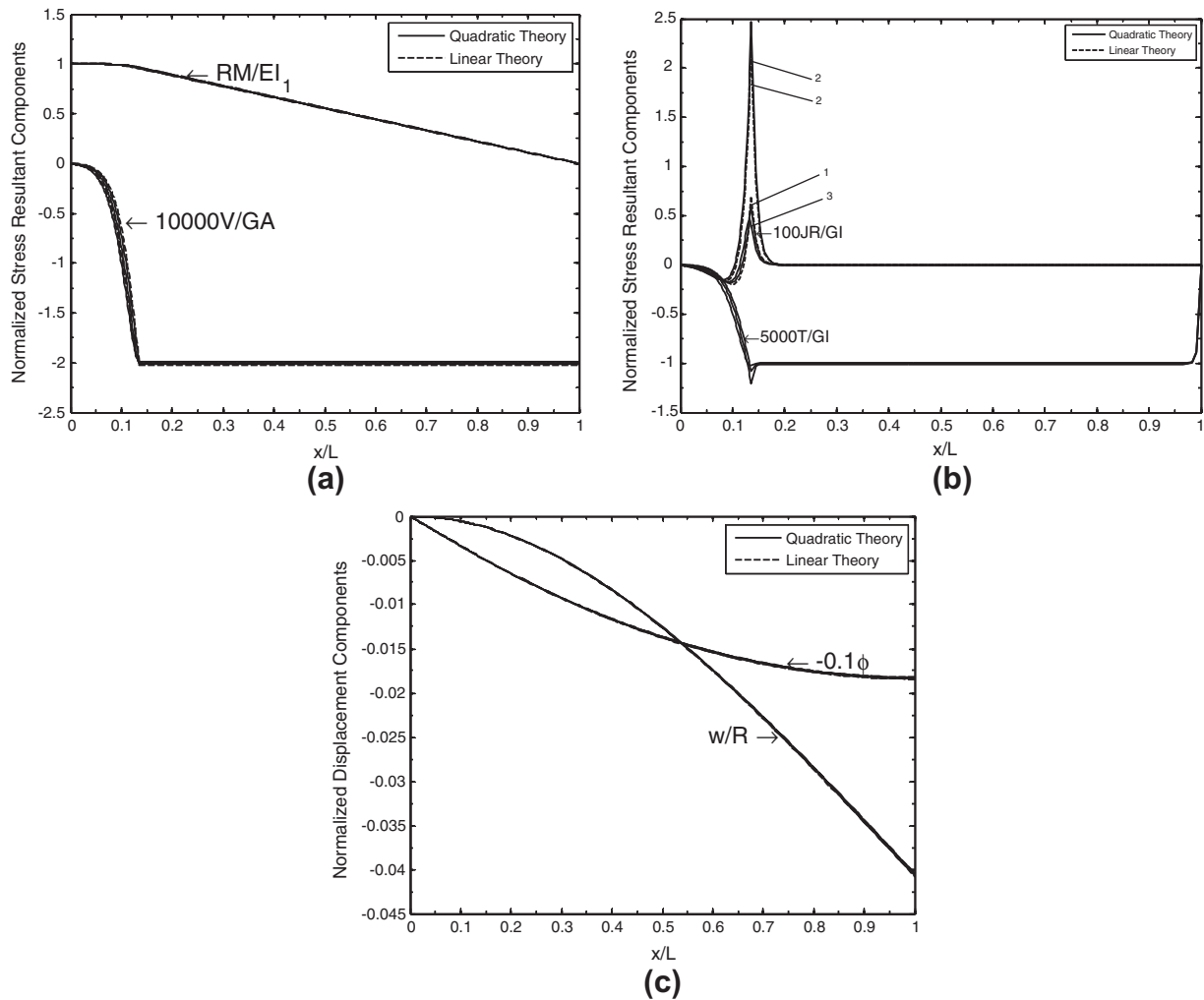


Fig. 16. Normalized stress resultants and displacement components, w and ϕ , for the five cases in Fig. 14: (a) V and M , (b) T and J , and (c) w and ϕ .

smooth bodies, the primary example being the so-called Hertz pressure. In the case of both higher order beam theories presented in this paper, more monomials in the transverse component of the displacement vector field are included. These functions can be used to achieve this zero pressure result, but require compromising the integrity of the beam formulation through the introduction of a discontinuity of one of these extra functions, i.e. ψ and β .

The pressure profiles presented in Fig. 14 include three variants of the quadratic theory, two variants of the linear theory and the plane elasticity solution for the case of an isotropic material ($\nu = 0.3$). The three different variants of the quadratic theory are: (1) the solution that is consistent with the beam formulation, which enforces continuity of all essential and natural quantities of the formulation, (2) one that enforces the continuity of the pressure by making ψ discontinuous and (3) one that enforces the continuity of the pressure at the cost of making β discontinuous at the edge of contact. Likewise, the variants of the linear theory are the solution that is consistent with the beam formulation, which enforces continuity of all essential and natural quantities, and the one that enforces the continuity of the pressure at the cost of making ψ discontinuous. It is clear that the pressure distributions are sensitive to both the representation of the displacement field and the manner in which a continuous pressure is enforced. In this special case of an isotropic beam the quadratic theory with β discontinuous and contact pressure continuous is the closest to the elasticity. However, based only on this special case, a conclusion cannot be made.

As stated above, forcing the pressure to drop to zero at the edge of contact requires a discontinuity in a function that should be continuous. This is illustrated in Fig. 15(a) and (b), which show the normalized displacement components, ψ and β , for the variants in Fig. 14. It is observed that cases “2” are discontinuous in Fig. 15(a), while case “3” is discontinuous in Fig. 15(b). The effect of the various enforcements on other quantities is illustrated in Fig. 16. In Fig. 16(a) the stress resultants V and M are presented, in Fig. 16(b) the secondary stress resultants, J and T , which show some change, are presented, and in Fig. 16(c) the displacement components, w and ϕ , which show very little change, are presented.

6. Conclusions

Two different higher order beam theories which account for transverse normal displacement as either linear or quadratic were derived using the principle of virtual work. These theories were applied to the problem of contact of a thin straight continuum strip with a circular smooth rigid surface with a focus on the effect of transverse normal deformation on the contact pressure. Examples showed that this effect is especially significant for beams with low transverse stiffness. In many cases the difference in pressure prediction between the linear and quadratic theories was significant, indicating a high degree of sensitivity of pressure to the transverse normal deformation.

The behavior of the contact stress at the edge of contact was studied in detail. It was shown that while the higher order theories

have the ability to force the pressure to drop to zero, boundary conditions resulting from the principle of virtual work must be violated to accomplish this. Furthermore, it was shown that the contact pressure is very sensitive to the method of enforcing this result.

It was demonstrated that for the same deflection, the constrained theories always overestimate the stress resultants and loads as compared to plane elasticity. Consistent with this, the more relaxed the theory, i.e., the higher the order of the theory, the less overestimated the results are.

It was noticed that when the shearing mode of deformation prevails, cross-sectional warping becomes important in the accurate prediction of contact stresses. This can be achieved by including more monomials in the polynomial expansion of the axial component of the displacement vector direction or it can also be tuned by the means of shear correction factors.

Finally, the present derived higher order beam theories can be a useful tool in solving problems of thin continua that involve surface constraints and contact problems.

Acknowledgements

This study was supported by a NIST/ATP grant. The Clemson authors gratefully acknowledge receiving support through the Michelin Americas Research and Development Corporation.

References

- Chen, J.-S., 2011. On the contact behavior of a buckled Timoshenko beam constrained laterally by a plane wall. *Acta Mech.* 222, 225–232.
- Cowper, G.R., 1966. The shear coefficient in Timoshenko's beam theory. *ASME J. Appl. Mech.* 33, 335–339.
- El-Abbasi, N., Meguid, S.A., 1999. Modeling frictional contact in shell structures using variational inequalities. *Finite Elem. Anal. Des.* 33, 317–334.
- Essenburg, F., 1975. On the significance of the inclusion of the effect of transverse normal strain in problems involving beams with surface constraints. *ASME J. Appl. Mech.* 42, 127–132.
- Gasmí, A., 2011. On the modeling of contact problems for curved and straight elastic thin continua with application to non-pneumatic tires. Ph.D. Dissertation, Clemson Univ., Clemson, USA.
- Gasmí, A., Joseph, P.F., Rhyne, T.B., Cron, S.M., 2011. Closed-form solution of a shear deformable, extensional ring in contact between two rigid surfaces. *Int. J. Solids Struct.* 48, 843–853.
- Gasmí, A., Joseph, P.F., Rhyne, T.B., Cron, S.M., 2012. Development of a two-dimensional model of a compliant non-pneumatic tire. *Int. J. Solids Struct.* 49, 1723–1740.
- Hodges, D.H., 2003. Contact stress from asymptotic Reissner–Mindlin plate theory. *AIAA J.* 41, 329–331.
- Johnson, K.L., 1985. *Contact Mechanics*. Cambridge Univ. Press, Cambridge.
- Keer, L.M., Silva, M.A.G., 1970. Bending of a cantilever brought gradually into contact with a cylindrical supporting surface. *Int. J. Mech. Sci.* 12, 751–760.
- Naghdi, P.M., Rubin, M.B., 1989. On the significance of normal cross-sectional extension in beam theory with application to contact problems. *Int. J. Solids Struct.* 25, 249–265.